

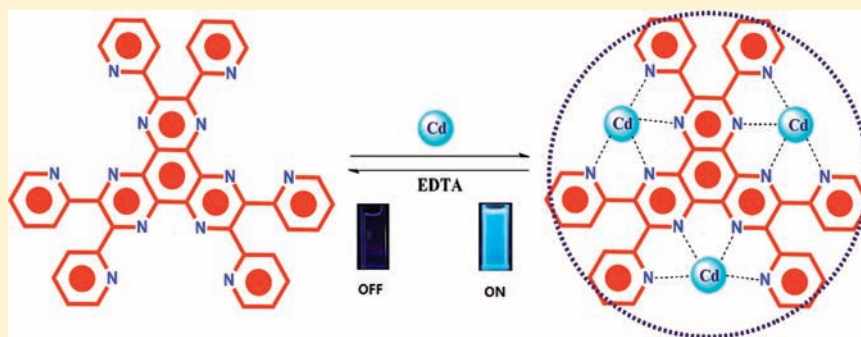
## A Highly Selective On/Off Fluorescence Sensor for Cadmium(II)

Qiang Zhao, Rui-Fang Li, Sheng-Kai Xing, Xiu-Ming Liu, Tong-Liang Hu, and Xian-He Bu\*

Department of Chemistry and Tianjin Key Lab on Metal and Molecule-based Material Chemistry, Nankai University, Tianjin 300071, China

Supporting Information

## ABSTRACT:



A polypyridyl ligand, 2,3,6,7,10,11-hexakis(2-pyridyl)dipyrazino[2,3-*f*:2',3'-*h*]quinoxaline (HPDQ), was found to have excellent fluorescent selectivity for  $\text{Cd}^{2+}$  over many other metal ions ( $\text{K}^+$ ,  $\text{Na}^+$ ,  $\text{Ca}^{2+}$ ,  $\text{Mg}^{2+}$ ,  $\text{Mn}^{2+}$ ,  $\text{Fe}^{2+}$ ,  $\text{Ni}^{2+}$ ,  $\text{Co}^{2+}$ ,  $\text{Cu}^{2+}$ ,  $\text{Ag}^+$ ,  $\text{Hg}^{2+}$ ,  $\text{Zn}^{2+}$ , and  $\text{Cr}^{3+}$ ) based on the intramolecular charge-transfer mechanism, which makes HPDQ a potential fluorescence sensor or probe for  $\text{Cd}^{2+}$ . An obvious color change between HPDQ and HPDQ +  $\text{Cd}^{2+}$  can be visually observed by the naked eye. The structure of the complex HPDQ-Cd has been characterized by X-ray crystallography. Density functional theory calculation results on the HPDQ and HPDQ-Cd complexes could explain the experimental results.

## INTRODUCTION

Cadmium is widely used in industry, agriculture, and many other fields.<sup>1</sup> Recently, serious environmental and health problems caused by  $\text{Cd}^{2+}$  make it in great need for the development of methods to detect and monitor cadmium levels.<sup>2,3</sup> Because of their simplicity and high sensitivity, fluorescence probes are powerful tools to monitor in vitro and/or in vivo biologically relevant species such as metal ions.<sup>4,5</sup> The challenge in developing a fluorescence sensor is to enhance and improve the induced signal when a particular target binds to the probe.<sup>6</sup> As we know, many synthetic sensors exhibiting fluorescent response to  $\text{Cd}^{2+}$  have already been found;<sup>7</sup> however, because  $\text{Cd}^{2+}$  and  $\text{Zn}^{2+}$  have very similar chemical properties, most of these sensors can also respond to  $\text{Zn}^{2+}$ .<sup>8</sup> Hence, it has been a great challenge to develop a  $\text{Cd}^{2+}$ -selective fluorescence sensor that can discriminate  $\text{Cd}^{2+}$  from  $\text{Zn}^{2+}$  and other metal ions, and now there are already some good cadmium fluorescence sensors showing fair selectivity over  $\text{Zn}^{2+}$  ions,<sup>9</sup> but a highly selective  $\text{Cd}^{2+}$  sensor is still in great need for further exploration.

In our extended efforts to design and synthesize new metal complexes with interesting structures and advanced functions,<sup>10</sup> we report herein our new discovery that a  $\pi$ -conjugated polydentate ligand, 2,3,6,7,10,11-hexakis(2-pyridyl)dipyrazino[2,3-*f*:2',3'-*h*]quinoxaline (HPDQ)<sup>11</sup> (see Chart 1), shows excellent  $\text{Cd}^{2+}$  selectivity over many other metal ions including  $\text{Zn}^{2+}$ ,

which was confirmed both experimentally and theoretically [by density functional theory (DFT) calculations].

## EXPERIMENTAL SECTION

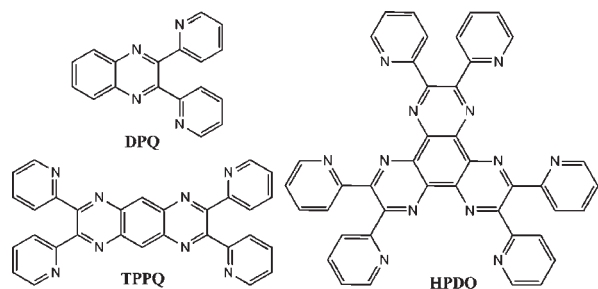
**Materials and General Methods.** All of the starting materials for synthesis were commercially available and were used as received. All of the solvents used for titration measurements were purified by standard procedures. The HPDQ ligand<sup>11</sup> was prepared according to the procedures described in the Supporting Information. The <sup>1</sup>H NMR spectrum was measured in  $\text{CDCl}_3$  at 25 °C with a Varian Unity Plus 400 MHz NMR spectrometer. Elemental analyses (C, H, and N) were performed on a Perkin-Elmer 240C analyzer. IR spectra were measured on a TENSOR 27 OPUS Fourier transform infrared (FT-IR) spectrometer (Bruker) using KBr disks dispersed with sample powders in the 4000–400  $\text{cm}^{-1}$  range. UV–vis absorption spectra were measured with a Hitachi U-3010 UV–vis spectrophotometer. Fluorescence spectra were recorded at room temperature on a Varian Cary Eclipse fluorescence spectrometer.

**Preparation of Fluorometric Titration Solutions.** Solutions (0.015 M) of metal ions ( $\text{K}^+$ ,  $\text{Na}^+$ ,  $\text{Ca}^{2+}$ ,  $\text{Mg}^{2+}$ ,  $\text{Mn}^{2+}$ ,  $\text{Fe}^{2+}$ ,  $\text{Ni}^{2+}$ ,  $\text{Co}^{2+}$ ,  $\text{Cu}^{2+}$ ,  $\text{Ag}^+$ ,  $\text{Hg}^{2+}$ ,  $\text{Cd}^{2+}$ ,  $\text{Zn}^{2+}$ , and  $\text{Cr}^{3+}$ ) were prepared in acetonitrile. The concentration of HPDQ in the fluorescence titration tests was

Received: April 20, 2011

Published: September 12, 2011

Chart 1


**Table 1. Crystal Data and Structure Refinement Parameters for Complexes HPDQ, HPDQ-Cd, and HPDQ-Zn**

	HPDQ	HPDQ-Cd	HPDQ-Zn
chemical formula	C <sub>84</sub> H <sub>48</sub> N <sub>24</sub> O <sub>3</sub>	C <sub>42</sub> H <sub>24</sub> Cd <sub>4</sub> N <sub>20</sub> O <sub>32</sub>	C <sub>84</sub> H <sub>48</sub> Zn <sub>8</sub> N <sub>40</sub> O <sub>68</sub>
fw	1441.46	1770.41	3228.58
space group	triclinic	monoclinic	triclinic
<i>a</i> /Å	20.138(4)	22.675(5)	13.735(3)
<i>b</i> /Å	13.745(6)	15.860(3)	16.380(3)
<i>c</i> /Å	25.279(5)	18.331(4)	16.529(3)
<i>α</i> /deg	90.00	90.00	63.89(3)
<i>β</i> /deg	101.53(3)	110.86(3)	89.91(3)
<i>γ</i> /deg	90.00	90.00	89.91(3)
<i>V</i> /Å <sup>3</sup>	6856(4)	6160(2)	79.40(3)
<i>Z</i>	4	4	1
<i>D</i> /g cm <sup>-3</sup>	1.396	1.909	1.640
<i>μ</i> /mm <sup>-1</sup>	0.091	1.471	1.556
<i>T</i> /K	293(2)	293(2)	293(2)
<i>R</i> <sup>a</sup> / <i>wR</i> <sup>b</sup>	0.0586/0.1849	0.0543/0.1354	0.0880/0.2933

<sup>a</sup>  $R1 = \sum ||F_o| - |F_c|| / \sum |F_o|$ . <sup>b</sup>  $wR2 = [\sum [w(F_o^2 - F_c^2)^2] / \sum w(F_o^2)^2]^{1/2}$ .

$5 \times 10^{-5}$  M with CH<sub>2</sub>Cl<sub>2</sub>/CH<sub>3</sub>CN (1:9, v/v) as the solvent. During titration, metal ions were added into a solution of HPDQ (3 mL) using a microinjector, and the whole volume of HPDQ and metal ions could be considered as 3 mL because the volume of the metal ions could be ignored compared to that of HPDQ. After stirring, the fluorescence spectra were recorded. For all of the measurements, excitation and emission slit widths were 5 nm.

**Synthesis of HPDQ-Cd.** In a tube, CH<sub>2</sub>Cl<sub>2</sub>/CH<sub>3</sub>CN (1:1, v/v; 10 mL) was carefully layered over a CH<sub>2</sub>Cl<sub>2</sub> (3 mL) solution of HPDQ (0.05 mmol) as a buffer layer, over which a solution of Cd(NO<sub>3</sub>)<sub>2</sub>·4H<sub>2</sub>O (0.15 mmol) in CH<sub>3</sub>CN (3 mL) was carefully added. This was left undisturbed at room temperature, and brown block-shaped crystals were harvested after about 3 weeks. FT-IR (KBr pellets, cm<sup>-1</sup>): 3421(m), 3133(s), 2361(s), 2341(s), 2170(w), 1653(m), 1591(w), 1559(w), 1399(s), 1241(w), 1171(w), 1029(w), 822(w), 792(w), 699(m), 566(w). Anal. Calcd for C<sub>42</sub>H<sub>24</sub>Cd<sub>4</sub>N<sub>20</sub>O<sub>32</sub>: C, 28.49; H, 1.37; N, 15.82. Found: C, 28.11; H, 1.69; N, 16.15.

**Synthesis of HPDQ-Zn.** In a tube, CH<sub>2</sub>Cl<sub>2</sub>/CH<sub>3</sub>CN (1:1, v/v; 10 mL) was carefully layered over a CH<sub>2</sub>Cl<sub>2</sub> (3 mL) solution of HPDQ (0.05 mmol) as a buffer layer, over which a solution of Zn(NO<sub>3</sub>)<sub>2</sub>·6H<sub>2</sub>O (0.15 mmol) in CH<sub>3</sub>CN (3 mL) was carefully added. This was left undisturbed at room temperature, and dark-brown block-shaped crystals were harvested after about 4 weeks. FT-IR (KBr pellets, cm<sup>-1</sup>): 3448(m), 3134(m), 1763(w), 1653(m), 1602(m), 1385(s), 1240(m), 1163(m), 1022(w), 826(m), 788(w), 753(w), 696(w), 602(w), 562(m).

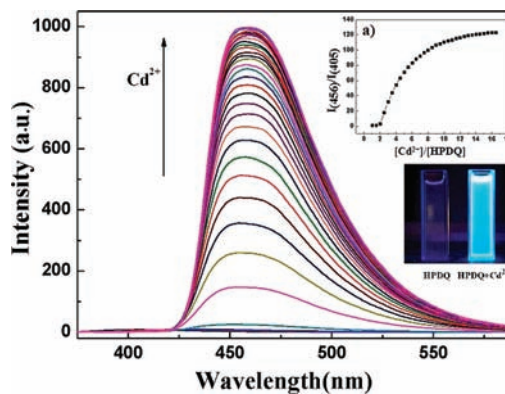


**Figure 1.** Fluorescence emission spectra ( $\lambda_{\text{ex}} = 300$  nm) of HPDQ ( $5 \times 10^{-5}$  mol L<sup>-1</sup>) in CH<sub>2</sub>Cl<sub>2</sub>/CH<sub>3</sub>CN (1:9, v/v, 3 mL) upon the addition of Cd<sup>2+</sup> (0, 0.5, 1, 1.5, 2, 2.5, 3, 3.5, 4, 4.5, 5, 5.5, 6, 6.5, 7, 7.5, 8, 8.5, 9, 9.5, 10, 10.5, 11, 11.5, 12, 12.5, 13, 13.5, 14, 14.5, 15, 15.5, and 16 equiv). The excitation and emission slit widths were 5 nm. Inset: (a) Ratiometric calibration curve  $I_{456 \text{ nm}}/I_{405 \text{ nm}}$  as a function of  $[Cd^{2+}]/[HPDQ]$ . The photograph was taken under a hand-held UV-vis (365 nm) lamp.

Anal. Calcd for C<sub>84</sub>H<sub>48</sub>Zn<sub>8</sub>N<sub>40</sub>O<sub>68</sub>: C, 31.25; H, 1.50; N, 17.35. Found: C, 30.91; H, 1.89; N, 17.67.

**X-ray Data Collection and Structure Determinations.** Single-crystal X-ray diffraction data for HPDQ was collected on a SCX-Mini diffractometer at 293(2) K, while complexes HPDQ-Cd and HPDQ-Zn were collected on a Rigaku RAXIS-RAPID diffractometer at 293(2) K with Mo K $\alpha$  radiation ( $\lambda = 0.71073$  Å) in  $\omega$ -scan mode. The program SAINT<sup>12</sup> was used for integration of the diffraction profiles. All of the structures were solved by direct methods using the SHELXS program of the SHELXTL package and refined by full-matrix least-squares methods with SHELXL (semiempirical absorption corrections were applied using the SADABS program).<sup>13</sup> Metal atoms in each complex were located from *E* maps, and other non-H atoms were located in successive difference Fourier syntheses and refined with anisotropic thermal parameters on *F*<sup>2</sup>. The H atoms of the ligands were generated theoretically on the specific atoms and refined isotropically with fixed thermal factors. Detailed crystallographic data are summarized in Table 1.

**Theoretical Calculations.** Theoretical investigations on the HPDQ and HPDQ-Cd complexes were performed by the Gaussian03 program package<sup>14</sup> and the B3LYP<sup>15</sup> method. We used the LANL2DZ<sup>16</sup> basis set and pseudopotential on Cd atoms, and the 3-21G\* basis set was used on all other atoms. The geometrical structures of HPDQ and HPDQ-Cd were fully optimized. The optimized structure of the HPDQ-Cd complex was very close to its single-crystal X-ray structure (see the parameters listed in Table S1 in the Supporting Information). All of the properties including the UV-vis [obtained by time-dependent DFT (TD-DFT)<sup>17</sup> calculations] and IR spectra were calculated at the same level based on the optimized structures.

## RESULTS AND DISCUSSION

**Fluorescence Titration.** The fluorescence titration experiments were carried out in CH<sub>2</sub>Cl<sub>2</sub>/CH<sub>3</sub>CN (1:9, v/v), and the fluorescence titration results of HPDQ toward Cd<sup>2+</sup> are shown in Figure 1. Compared with the weak fluorescence at 405 nm ( $\lambda_{\text{ex}} = 300$  nm; Figure S1 in the Supporting Information) of the free HPDQ, it is notable that a new emission peak at 456 nm appeared, and the fluorescence intensity increased strikingly after the addition of Cd<sup>2+</sup> ions. Clearly, the emission color of the solution changed from dark to bright blue after Cd<sup>2+</sup> ions were added.

A comparison of the  $I_{456\text{ nm}}/I_{405\text{ nm}}$  ratio of the fluorescence intensity after and before the addition of  $\text{Cd}^{2+}$  exhibits an approximate 126-fold enhancement; the fluorescence quantum yield is 0.048,<sup>18</sup> and the association constants of HPDQ with Cd were obtained as  $K_{\text{Cd1}} = 3.7 \times 10^4$ ,  $K_{\text{Cd2}} = 1.2 \times 10^4$ , and  $K_{\text{Cd3}} = 4.1 \times 10^3$ , respectively, by a reported method.<sup>19</sup> The change of the fluorescence may originate from the following: (a) The intramolecular charge-transfer (ICT) effect caused by  $\text{Cd}^{2+}$  coordination, in other words, the coordination of  $\text{Cd}^{2+}$  to N atoms, will reduce the electron-withdrawing ability of the N atoms and lower the electron density of HPDQ.<sup>20</sup> This was confirmed quantitatively by the DFT calculation results, which will be discussed later. (b) The increase of the conjugate effect, that is, the formation of the complex, may have enhanced the HPDQ conjugate effect, so the solution exhibits stronger fluorescence with enhanced plane rigidity.<sup>21,22</sup> Meanwhile, we also noticed that, in Figure S1 in the Supporting Information, the fluorescent intensity has a small change and a small red shift when the addition of  $\text{Cd}^{2+}$  is less than 1 equiv. This may be because when less than 1 equiv of  $\text{Cd}^{2+}$  is added to HPDQ (at a low concentration), HPDQ and  $\text{Cd}^{2+}$  could not form a stable complex. Nearly all of the fluorescence intensity of the solution came from HPDQ, so the fluorescence intensity of the solution changed very little. As the concentration of  $\text{Cd}^{2+}$  is increased and when the addition of  $\text{Cd}^{2+}$  is near about 2 equiv, a few stable complex species might form and the fluorescence intensity of the solution increases slowly. When  $\text{Cd}^{2+}$  is added to about 3 equiv of HPDQ, most of HPDQ and  $\text{Cd}^{2+}$  could form a stable complex in the solution, the new luminescent substance formed. Under the effect of the ICT effect and the conjugate effect, all of the fluorescence intensity of the solution may come from the new luminescent substance. So, the new emission peak at 456 nm appeared, and the fluorescence intensity increased strikingly. The solution behavior of this system is complicated and will be further studied.

Although 2,3-bis(2-pyridyl)quinoxaline (DPQ) and 2,3,7,8-tetrakis(2-pyridyl)pyrazino[2,3-g]quinoxaline (TPPQ)<sup>10a</sup> have coordination structural units similar to those of HPDQ, experimental results showed that the fluorescence properties of DPQ and TPPQ are very different from those of HPDQ. The fluorescence intensity of DPQ increased only slightly, and the fluorescence of TPPQ was quenched with increased concentration of  $\text{Cd}^{2+}$  (Figure S2 in the Supporting Information). This indicated that the formation of the planar trinuclear structure (which will be discussed later in the X-ray structure part) should be the key point for enhancement of the fluorescence.

The UV–vis spectrum of HPDQ exhibits two strong absorption peaks at 308 and 343 nm, respectively (Figure S3a in the Supporting Information). The addition of the first 1 equiv of  $\text{Cd}^{2+}$  causes the absorption peaks to red shift, and the intensity of the maximum absorption peak decreased a little. When the concentration of  $\text{Cd}^{2+}$  was increased, two large absorption peaks appeared at 360 and 395 nm, and the red shift was about 52 nm (Figure S3b in the Supporting Information).

**Selection and Competition Experiments.** The fluorescence emission of HPDQ changes when different metal ions are bound, and the detection of metal ions with HPDQ was carried out in  $\text{CH}_2\text{Cl}_2/\text{CH}_3\text{CN}$  (1:9, v/v). As shown in Figure S4 in the Supporting Information, HPDQ itself shows quite weak emission at around 405 nm. Among all of the metal ions investigated, HPDQ shows unexpected high selectivity to  $\text{Cd}^{2+}$ , while fluorescence intensity changes were hardly observed when  $\text{K}^+$ ,  $\text{Na}^+$ ,

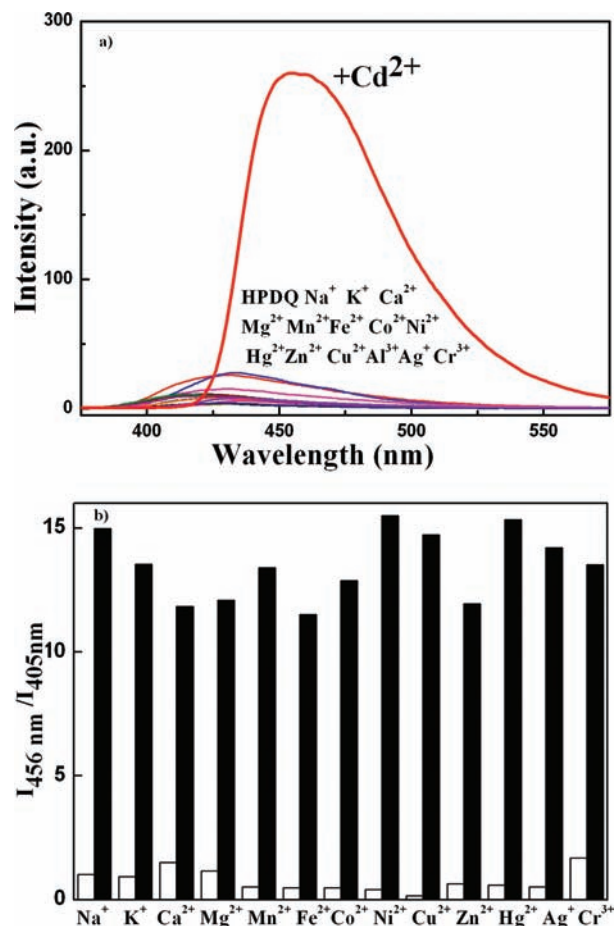


**Figure 2.** (a) Fluorescence emission spectra ( $\lambda_{\text{ex}} = 300\text{ nm}$ ) of HPDQ ( $5 \times 10^{-5}\text{ mol L}^{-1}$ ) in the presence of different metal ions (3 equiv) in the  $\text{CH}_2\text{Cl}_2/\text{CH}_3\text{CN}$  (1:9, v/v). The excitation and emission slit widths were 5 nm. (b) Fluorescence responses of HPDQ ( $5 \times 10^{-5}\text{ mol L}^{-1}$ ) to various metal ions in  $\text{CH}_2\text{Cl}_2/\text{CH}_3\text{CN}$  (1:9, v/v; 3 mL). The bars represent the final fluorescence intensity at 456 nm ( $I$ ) over the original emission at 405 nm ( $I_0$ ). White bars represent the addition of 3 equiv of different metal ions to HPDQ. Black bars represent the subsequent addition of 3 equiv of  $\text{Cd}^{2+}$  to the solution.

$\text{Mg}^{2+}$ ,  $\text{Mn}^{2+}$ ,  $\text{Fe}^{2+}$ ,  $\text{Ni}^{2+}$ ,  $\text{Co}^{2+}$ ,  $\text{Cu}^{2+}$ ,  $\text{Ag}^+$ ,  $\text{Hg}^{2+}$ , or  $\text{Zn}^{2+}$  was added to the solution, except the addition of  $\text{Ca}^{2+}$  or  $\text{Cr}^{3+}$  does induce slight fluorescence enhancements (Figure S4 in the Supporting Information). Moreover, the addition of  $\text{Cd}^{2+}$  not only enhances the fluorescence emission significantly but also changes the solution emission color from dark to bright blue. As shown in Figure 1, the emission color change is very obvious upon the addition of  $\text{Cd}^{2+}$ , while there was hardly any effect on the fluorescence of HPDQ when other metal ions were added (Figure 2a). This means that HPDQ can be used to distinguish  $\text{Cd}^{2+}$  from other common metal ions. Compared with HPDQ, the experimental results show that neither DPQ nor TPPQ has selectivity to  $\text{Cd}^{2+}$  (Figure S5 in the Supporting Information).

Binding competition experiments were also conducted for HPDQ (Figure 2b). When  $\text{Cd}^{2+}$  was added into a solution of HPDQ in the presence of other ions, a prominent increase of the emission appeared. The results indicate that HPDQ shows excellent selectivity to  $\text{Cd}^{2+}$  and might be used to detect  $\text{Cd}^{2+}$  even with the coexistence of other common metal ions.

**Reversibility.** The recognition process of  $\text{Cd}^{2+}$  by HPDQ was found to be reversible. This was demonstrated by the subsequent addition of an equal amount of an ethylenediaminetetraacetic acid (EDTA) aqueous solution into the glowing HPDQ- $\text{Cd}^{2+}$  solution, which can almost recover the original emission of HPDQ (Figure 3). From the above phenomenon, we think HPDQ could probably be used as a fluorescence switch.

**Discrimination between  $\text{Cd}^{2+}$  and  $\text{Zn}^{2+}$ .** As we know, the discrimination between  $\text{Cd}^{2+}$  and  $\text{Zn}^{2+}$  is very difficult because they have very similar chemical properties. However, HPDQ makes it possible and provides an easy way to distinguish  $\text{Cd}^{2+}$  from  $\text{Zn}^{2+}$  by the naked eye. As illustrated in Figure 4, the color change of the solution is very obvious after  $\text{Cd}^{2+}$  or  $\text{Zn}^{2+}$  is added: the solution of free HPDQ is nearly colorless, while after  $\text{Cd}^{2+}$  is added, the color of the solution changes to light yellow and gives a bright-blue fluorescence under a hand-held UV-vis (365 nm) lamp. However, after  $\text{Zn}^{2+}$  is added, the color of the solution changes to reddish-brown and no fluorescence is observed under the same lamp. All of the above-mentioned evidence shows that it is very easy to discriminate  $\text{Zn}^{2+}$  and  $\text{Cd}^{2+}$  by HPDQ.

**Crystal Structures.** In order to understand the reason why there are such large different phenomena after reaction with  $\text{Cd}^{2+}$  and  $\text{Zn}^{2+}$ , respectively, we studied the crystal structures of the two complexes (see Figure 5). As shown in Chart 1, HPDQ has two types of N atoms. In order to distinguish them easily, we named them pyridyl N and dipyrzino N atoms.

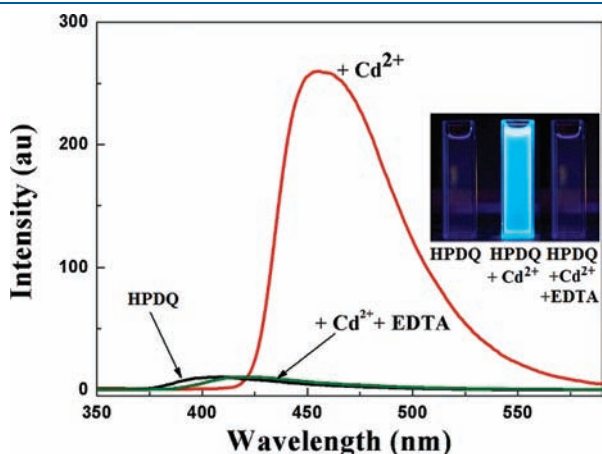


**Figure 3.** Fluorescence reversibility of HPDQ upon the detection of  $\text{Cd}^{2+}$ . Inset: Visual fluorescent change of HPDQ after the addition of  $\text{Cd}^{2+}$  and the sequential addition of an EDTA aqueous solution, respectively. The photographs were taken under a hand-held UV-vis (365 nm) lamp.

We can see that HPDQ and  $\text{Cd}^{2+}$  can form a rigid trinuclear structure with 1:3 stoichiometry (Figures S5a and S6a in the Supporting Information), which crystallizes in the monoclinic space group  $C2/c$ , and the asymmetric unit of this complex consists of half of a HPDQ ligand and two  $\text{Cd}^{2+}$  ions ( $\text{Cd1}$  and  $\text{Cd2}$ ).  $\text{Cd1}$  is coordinated by three O atoms ( $\text{O4}$ ,  $\text{O6}$ , and  $\text{O7}$ ) from  $\text{NO}_3^-$ , an O atom ( $\text{O3}$ ) from water, and two pyridyl N

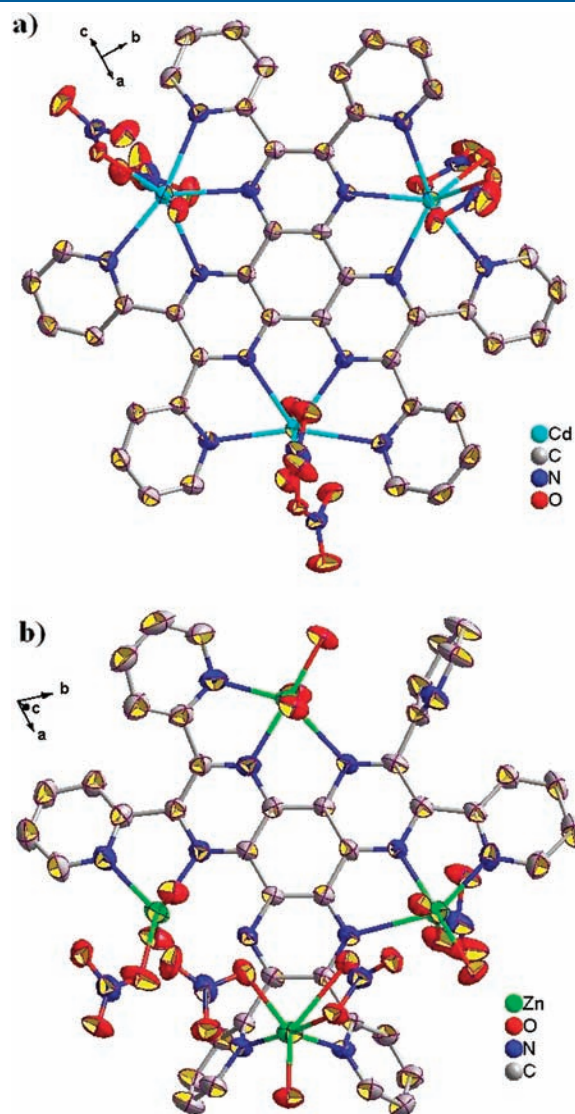


**Figure 5.** (a) Perspective thermal ellipsoid view of the single-crystal structures of (a) HPDQ- $\text{Cd}$  and (b) HPDQ- $\text{Zn}$  at 50% probability.

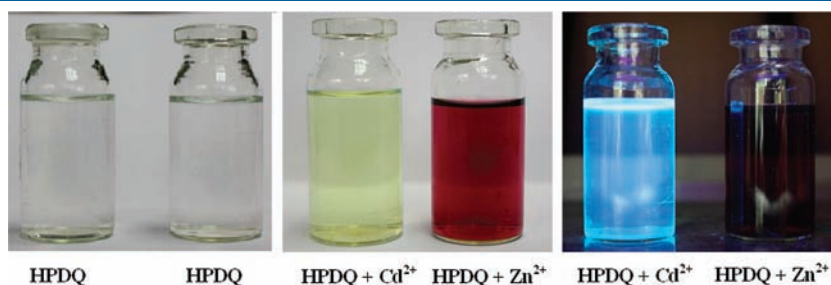


**Figure 4.** Color and fluorescence changes of HPDQ after  $\text{Cd}^{2+}$  or  $\text{Zn}^{2+}$  was added.

atoms (N1 and N4) and two dipyrazino N atoms (N2 and N3) of HPDQ, and Cd2 is coordinated by four O atoms (O1, O2, O1A, and O2A) from  $\text{NO}_3^-$  and two pyridyl N atoms (N5 and N5A) and two dipyrazino N atoms (N6 and N6A) of HPDQ. Cd–N bond distances are in the 2.418(4)–2.514(4) Å range, Cd–O bond distances are in the 2.297(4)–2.615(5) Å range, N–Cd–N angles are in the range of 63.68(13)–161.5(2)°, O–Cd–N angles are in the range of 79.41(17)–144.43(14)°, and O–Cd–O angles are in the range of 49.76(18)–157.45(18)°. Cd1, Cd1A, and Cd2 are connected to each other by HPDQ, forming a disk-shaped planar structure.

HPDQ–Zn (Figures S5b and S6b in the Supporting Information) is a tetranuclear complex that crystallizes in the triclinic space group  $P\bar{1}$ , in which the asymmetric unit consists of HPDQ and four Zn atoms (Zn1, Zn2, Zn3, and Zn4). Zn1 is coordinated by an O atom (O6) from  $\text{NO}_3^-$ , two O atoms (O7 and O8) from water, and one pyridyl N atom (N11) and two dipyrazino N atoms (N2 and N3) of HPDQ, and Zn2 is coordinated by three O atoms (O10, O11, and O13) from  $\text{NO}_3^-$ , one O atom (O29) from water, and two pyridyl N atoms (N9 and N10) of HPDQ, and Zn3 is coordinated by three O atoms (O30, O31, and O32) from water, and one pyridyl N atom (N7) and two dipyrazino N atoms (N1 and N6) of HPDQ, while Zn4 is coordinated by one O atom (O16) from  $\text{NO}_3^-$ , two O atoms (O18 and O19) from water, and one pyridyl N atom (N8) and one dipyrazino N atom (N5) of HPDQ. Zn–N bond distances are in the 2.117(5)–2.544(5) Å range, Zn–O bond distances are in the 1.998(6)–2.518 Å range, N–Zn–N angles are in the range of 74.2(2)–148.4(2)°, O–Zn–N angles are in the range of 87.8(2)–175.5(2)°, and O–Zn–O angles are in the range of 82.3(2)–169.9(3)°. Two N atoms (N4 and N12) of HPDQ do not participate in coordination (for crystal data, see Table 1).

Therefore, the structures of the two complexes are quite different, and this may be the main reason for their different fluorescent behaviors.

**Theoretical Studies.** The calculation results (see the Supporting Information for other calculation details) show that charges (the amount is 0.9e in Mulliken charge) are transferred from HPDQ to Cd in complex HPDQ–Cd. The charge on each N atom of the coordinated HPDQ increases by 0.1e (Mulliken charge) compared with free HPDQ. This strongly supports the above-mentioned ICT mechanism. Generally, a plane with rigid organic molecules exhibits stronger fluorescence because the planar structure can reduce the loss of energy through a radiationless pathway.<sup>21,22</sup> The theoretical optimization results of the HPDQ and HPDQ–Cd complexes show that HPDQ in the HPDQ–Cd complex becomes flatter than free HPDQ (the dihedral angle of the four atoms, which can represent the flatness of HPDQ, reduces from 46.65 to 20.86°), which means that HPDQ will become more rigid after coordination to  $\text{Cd}^{2+}$  (see Table S1 in the Supporting Information). No wonder the fluorescence of HPDQ increased dramatically after  $\text{Cd}^{2+}$  ions were added to its solution.

The calculated UV–vis spectra (Figure S7 in the Supporting Information) of the HPDQ (black curves) and HPDQ–Cd (red curves) complexes are similar to the spectra obtained by experiment. The main absorption peaks of the HPDQ and HPDQ–Cd complexes are located at 254 and 311 nm and 298 and 365 nm, respectively. The red shift of the calculated UV–vis spectrum is about 50 nm, which is almost the same as that of the experimental results (52 nm). Some of the differences between experimental and theoretical UV–vis spectra (45 nm) are perhaps caused by the solvent effects.

## CONCLUSION

We found that the polypyridyl compound HPDQ has excellent fluorescence selectivity for  $\text{Cd}^{2+}$  over many other metal ions including  $\text{Zn}^{2+}$ . The monitoring event could readily be observed under UV–vis light irradiation because the emission color changes intuitively from dark to bright blue. Theoretical calculation results can explain the fluorescence increment from HPDQ to HPDQ–Cd. Further studies are underway in our laboratory.

## ASSOCIATED CONTENT

**Supporting Information.** Experimental procedures and characterization data for the synthesis, crystal data, and calculated information and X-ray structural data for CCDC 791350 (HPDQ–Cd), 791351 (HPDQ–Zn), and 804615 (HPDQ) in CIF format. This material is available free of charge via the Internet at <http://pubs.acs.org>. The atomic coordinates for this structure have also been deposited with the Cambridge Crystallographic Data Centre. The coordinates can be obtained, upon request, from the Director, Cambridge Crystallographic Data Centre, 12 Union Road, Cambridge CB2 1EZ, U.K.

## AUTHOR INFORMATION

### Corresponding Author

\*E-mail: [buxh@nankai.edu.cn](mailto:buxh@nankai.edu.cn). Tel: +86-22-23502809. Fax: +86-22-23502458.

## ACKNOWLEDGMENT

We are thankful for financial supports from NSFC (Grants 21031002 and 51073079), the Natural Science Fund of Tianjin, China (Grant 10JCZDJC22100), and the 973 Program of China (2007CB815305).

## REFERENCES

- (1) For examples, (a) Chaney, R. L.; Ryan, J. A.; Li, Y. M.; Brown, S. L. In *Cadmium in Soils and Plants*; McLaughlin, M. J., Singh, B. R., Eds.; Kluwer: Boston, 1999; p 219. (b) Lyn Patrick, N. D. *Altern. Med. Rev.* **2003**, *8*, 106. (c) Pari, L.; Murugavel, P.; Sitasawad, S. L.; Kumar, K. S. *Life Sci.* **2007**, *80*, 650.
- (2) For examples, see: (a) Satarug, S.; Moore, M. R. *Environ. Health Perspect.* **2004**, *112*, 1099. (b) Jin, T.; Lu, J.; Nordberg, M. *Neurotoxicology* **1998**, *19*, 529. (c) Nordberg, M.; Nordberg, G. F. In *Heavy Metals in the Environment*; Sarkar, B., Ed.; Marcel Dekker: New York, 2002; p 231.
- (3) For examples, see: (a) Waisberg, M.; Joseph, P.; Hale, B. *Toxicology* **2003**, *192*, 95. (b) Waalkes, M. P. *J. Inorg. Biochem.* **2000**, *79*, 241. (c) Marnett, M.; Aragoni, M. C.; Arca, M.; Caltagirone, C.; Demartin, F.; Farruggia, G.; Filippo, G. D.; Devillanova, F. A.; Garau, A.; Isaia, F.; Lippolis, V.; Murgia, S.; Prodi, L.; Pintus, A.; Zaccheroni, N. *Chem.—Eur. J.* **2010**, *16*, 919.
- (4) For examples, see: (a) Tamanini, E.; Katewa, A.; Sedger, L. M.; Todd, M. H.; Watkinson, M. *Inorg. Chem.* **2009**, *48*, 319. (b) Li, H. R.; Cheng, W. J.; Wang, Y.; Liu, B. Y.; Zhang, W. J.; Zhang, H. J. *Chem.—Eur. J.* **2010**, *16*, 2125. (c) Liu, W. S.; Jiao, T. Q.; Li, Y. Z.; Liu, Q. Z.; Tan, M. Y.; Wang, H.; Wang, L. F. *J. Am. Chem. Soc.* **2004**, *126*, 2280.
- (5) (a) Tang, X. L.; Peng, X. H.; Dou, W.; Mao, J.; Zheng, J. R.; Qin, W. W.; Liu, W. S.; Chang, J.; Yao, X. J. *Org. Lett.* **2008**, *10*, 3653. (b) Komatsu, K.; Urano, Y.; Kojima, H.; Nagano, T. *J. Am. Chem. Soc.* **2007**, *129*, 13447.
- (6) (a) Ravikumar, I.; Ghosh, P. *Inorg. Chem.* **2011**, *50*, 4229. (b) DeSilva, A. P.; Gunaratne, H. Q. N.; Gunnlaugsson, T.; Huxley, A. J. M.; McCoy, C. P.; Rademacher, J. T.; Rice, T. E. *Chem. Rev.* **1997**,

97, 1515. (c) Drewry, J. A.; Gunning, P. T. *Coord. Chem. Rev.* **2011**, 255, 459. (d) Domaille, D. W.; Que, E. L.; Chang, C. J. *Nat. Chem. Biol.* **2008**, 4, 168. (e) Basabe-Desmonts, L.; Reinhoudt, D. N.; Crego-Calama, M. *Chem. Soc. Rev.* **2007**, 36, 993.

(7) For examples, see: (a) Cockrell, G. M.; Zhang, G.; VanDerveer, D. G.; Thummel, R. P.; Hancock, R. D. *J. Am. Chem. Soc.* **2008**, 130, 1420. (b) Nolan, E. M.; Ryu, J. W.; Jaworski, J.; Feazell, R. P.; Sheng, M.; Lippard, S. J. *J. Am. Chem. Soc.* **2006**, 128, 15517. (c) Komatsu, K.; Kikuchi, K.; Kojima, H.; Urano, Y.; Nagano, T. *J. Am. Chem. Soc.* **2005**, 127, 10197. (d) Goldsmith, C. R.; Lippard, S. J. *Inorg. Chem.* **2006**, 45, 555. (e) Xue, L.; Li, G.; Liu, Q.; Wang, H.; Liu, C.; Ding, X.; He, S.; Jiang, H. *Inorg. Chem.* **2011**, 50, 3680. (f) Liu, Z. P.; Zhang, C. L.; He, W. J.; Yang, Z. H.; Gao, X.; Guo, Z. J. *Chem. Commun.* **2010**, 46, 6138. (g) Gunnlaugsson, T.; Lee, T. C.; Parkesh, R. *Org. Lett.* **2003**, 22, 4065.

(8) (a) Nolan, E. M.; Lippard, S. J. *Inorg. Chem.* **2004**, 43, 8310. (b) Aoki, S.; Kagata, D.; Shiro, M.; Takeda, K.; Kimura, E. *J. Am. Chem. Soc.* **2004**, 126, 13377. (c) Lim, N. C.; Schuster, J. V.; Porto, M. C. *Inorg. Chem.* **2005**, 44, 2018. (d) Parkesh, R.; Lee, T. C.; Gunnlaugsson, T. *Org. Biomol. Chem.* **2007**, 5, 310.

(9) (a) Cheng, T. Y.; Xu, Y. F.; Zhang, S. Y.; Zhu, W. P.; Qian, X. H.; Duan, L. P. *J. Am. Chem. Soc.* **2008**, 130, 16160. (b) Bao, Y. Y.; Liu, B.; Wang, H.; Du, F. F.; Bai, R. K. *Anal. Methods* **2011**, 3, 1274.

(10) (a) Bu, X. H.; Liu, H.; Du, M.; Wong, K. M. C.; Yam, V. W. W.; Shionoya, M. *Inorg. Chem.* **2001**, 40, 4143. (b) Bu, X. H.; Tong, M. L.; Chang, H. C.; Kitagawa, S.; Batten, S. R. *Angew. Chem., Int. Ed.* **2004**, 43, 192. (c) Bu, X. H.; Chen, W.; Lu, S. L.; Zhang, R. H.; Liao, D. Z.; Shionoya, M. *Angew. Chem., Int. Ed.* **2001**, 40, 320.

(11) (a) Xiao, Z. Y.; Zhao, X.; Jiang, X. K.; Li, Z. T. *Chem. Mater.* **2011**, 23, 1505. (b) Xiao, Z. Y.; Zhao, X.; Jiang, X. K.; Li, Z. T. *Langmuir* **2010**, 16, 13048.

(12) *SAINT Software Reference Manual*; Bruker AXS: Madison, WI, 1998.

(13) Sheldrick, G. M. *SHELXTL NT: Program for Solution and Refinement of Crystal Structures*, version 5.1; University of Göttingen: Göttingen, Germany, 1997.

(14) Frisch, M. J.; Trucks, G. W.; Schlegel, H. B.; Scuseria, G. E.; Robb, M. A.; Cheeseman, J. R.; Montgomery, J. A.; Vreven, J. T.; Kudin, K. N.; Burant, J. C.; Millam, J. M.; Iyengar, S. S.; Tomasi, J.; Barone, V.; Mennucci, B.; Cossi, M.; Scalmani, G.; Rega, N.; Petersson, G. A.; Nakatsuji, H.; Hada, M.; Ehara, M.; Toyota, K.; Fukuda, R.; Hasegawa, J.; Ishida, M.; Nakajima, T.; Honda, Y.; Kitao, O.; Nakai, H.; Klene, M.; Li, X.; Knox, J. E.; Hratchian, H. P.; Cross, J. B.; Adamo, C.; Jaramillo, J.; Gomperts, R.; Stratmann, R. E.; Yazyev, O.; Austin, A. J.; Cammi, R.; Pomelli, C.; Ochterski, J. W.; Ayala, P. Y.; Morokuma, K.; Voth, G. A.; Salvador, P.; Dannenberg, J. J.; Zakrzewski, V. G.; Dapprich, S.; Daniels, A. D.; Strain, M. C.; Farkas, O.; Malick, D. K.; Rabuck, A. D.; Raghavachari, K. J.; Foresman, B.; Ortiz, J. V.; Cui, Q.; Baboul, A. G.; Clifford, S.; Cioslowski, J.; Stefanov, B. B.; Liu, G.; Liashenko, A.; Piskorz, P.; Komaromi, I.; Martin, R. L.; Fox, D. J.; Keith, T.; Al-Laham, M. A.; Peng, C. Y.; Nanayakkara, A.; Challacombe, M. P.; Gill, M. W.; Johnson, B.; Chen, W.; Wong, M. W.; Gonzalez, C.; Pople, J. A. *Gaussian03*; Gaussian, Inc.: Pittsburgh, PA, 2003.

(15) (a) Lee, C. T.; Yang, W. T.; Parr, R. G. *Phys. Rev. B* **1988**, 37, 785. (b) Becke, A. D. *J. Chem. Phys.* **1993**, 98, 5648. (c) Foresman, J. B.; Frisch, A. *Exploring Chemistry with Electronic Structure Methods*, 2nd ed.; Gaussian, Inc.: Pittsburgh, PA, 1996. (d) Parr, R. G.; Yang, W. *Density Functional Theory of Atoms and Molecules*; Oxford University Press: New York, 1989.

(16) (a) Chiodo, S.; Russo, N.; Sicilia, E. *J. Chem. Phys.* **2006**, 125, 104107. (b) Hay, P. J.; Wadt, W. R. *J. Chem. Phys.* **1985**, 82, 270.

(17) Frisch, M. J.; Trucks, G. W.; Cheeseman, J. R. In *Recent Developments and Applications of Modern Density Functional Theory*; Seminario, J. M., Ed.; Elsevier: Amsterdam, The Netherlands, 1996; p 679.

(18) Casey, K. G.; Quitevis, E. L. *J. Phys. Chem.* **1988**, 92, 6590.

(19) (a) Connors, K. A. *Binding Constants*; Wiley: New York, 1987. (b) Valeur, B. *Molecular Fluorescence: Principles and Applications*; Wiley-

VCH: Weinheim, Germany, 2001. (c) Peng, X. J.; Du, J. J.; Fan, J. L.; Wang, J. Y.; Wu, Y. K.; Zhao, J. Z.; Sun, S. G.; Xu, T. *J. Am. Chem. Soc.* **2007**, 129, 1500. (d) Baruah, M.; Qin, W.; Vallée, R. A. L.; Beljonne, D.; Rohand, T.; Dehaen, W.; Boens, N. *Org. Lett.* **2005**, 7, 4377.

(20) (a) Yang, Z. H.; Yan, C. C.; Chen, Y. C.; Zhu, C. C.; Zhang, C. L.; Dong, X. D.; Yang, W. Q.; Guo, Z. J.; He, W. J. *Dalton Trans.* **2011**, 40, 2173. (b) Resch-Genger, U.; Li, Y. Q.; Bricks, J. L. *J. Phys. Chem. A* **2006**, 110, 10956.

(21) (a) Zhang, L. Y.; Zhang, J. P.; Lin, Y. Y.; Chen, X. M. *Cryst. Growth Des.* **2006**, 6, 1684. (b) Zheng, S. L.; Yang, J. H.; Yu, X. L.; Chen, X. M.; Wong, W. T. *Inorg. Chem.* **2004**, 43, 830.

(22) (a) Jiang, T.; Zhao, Y. F.; Zhang, X. M. *Inorg. Chem. Commun.* **2007**, 10, 1194. (b) Li, J. R.; Tao, Y.; Yu, Q.; Bu, X. H. *Chem. Commun.* **2007**, 15, 1527.